Shear-Induced Smectic Ordering as a Precursor of Crystallization in Isotactic Polypropylene

Liangbin Li and Wim H. de Jeu*

FOM-Institute for Atomic and Molecular Physics, Kruislaan 407, 1098 SJ Amsterdam, The Netherlands

Received December 20, 2002; Revised Manuscript Received April 15, 2003

ABSTRACT: Using in-situ small- and wide-angle X-ray scattering, we demonstrate that bundles with smectic ordering are produced by a step shear in a supercooled isotactic polypropylene melt. This occurs well before any formation of crystals. The period of the smectic mesophase is about 3.8 nm and depends neither on the shear rate nor on the temperature. During the subsequent crystallization, crystals grow epitaxially around the smectic filaments that provide nucleation sites. The period of the crystals is an order of magnitude larger than the smectic one. Finally, the smectic filaments also transform into crystals, which is accompanied by a slight increase of the period to 4 nm. A new picture of the shish-kebab structure is presented in which the initial smectic bundles, instead of extended-chain crystals, play the role of the shish, while crystals grow epitaxially around it as kebabs.

Introduction

For many years nucleation and growth as a stepwise process has dominated discussions about polymer crystallization.[1] In contrast to this view, Strobl[2] proposed a multistage process to explain polymer crystallization, while other authors concluded from X-ray scattering data to a spinodal-assisted crystallization process.[3−5] The picture of a multistage process can be traced back to 1967,[6,7] while Schultz proposed already a spinodal approach for orientated systems in 1981.[8] These ideas have in common that crystallization of polymers is preceded by an ordered precursor. Clearly structural information about such possible precursors is necessary to verify this hypothesis. In recent years this point has been subjected to an important and still open debate.[9−11] In the case of shear-induced crystallization so-called shish-kebab structures occur, in which oriented molecules serve as precursor of primary nucleation and form the shish.[12,13] After formation of the shish, the kebabs grow epitaxially around it. Such a two-step process potentially allows exploring primary nucleation by investigating the structure of the shish. Though hard knowledge is still limited, the common picture assumes that the shish consists of (defective) extended-chain crystals.[14−17] A recent computer simulation shows that even a single prealigned molecular chain can induce the shish-kebab structure.[18] Further knowledge about the nature of the shish is of importance not only for our fundamental understanding of polymer crystallization but also for the industrial processing of polymers.

To explore the structure of the shish, it would be helpful if a specific structural marker, for instance a liquid crystalline phase, could be associated with it. Isotactic polypropylene (iPP) potentially provides such a possibility. In addition to three crystal modifications with a 3-fold helical conformation of the chain, called α, β, and γ,[19] also a smectic mesophase has been reported in rapidly quenched[20,21] and cold plasma-treated samples.[22] Left- and right-handed helices are randomly distributed in this mesophase, which makes it structurally suitable to act as a type of precursor. The observation of such an effect would provide important support for the new multistep crystallization schemes. However, although both rapid-quenched and step-sheared iPP have been extensively studied,[23−30] clear evidence about any precursor as well as any possible relation with crystallization is still absent.

In this paper, we show from small- and wide-angle X-ray scattering that smecticlike layering can be produced by a step shear in a supercooled iPP melt, as evidenced by a scattering peak around $q = 1.67$ nm^{-1}. The smectic bundles acts as precursor by providing nucleation sites promoting the growth of crystals, though it is rather difficult for them to become crystalline themselves. A new picture of the shish-kebab structure is proposed in which, instead of extended-chain crystals, the initial smectic bundles act as the shish and crystals grow epitaxially around it as the kebabs.

Experimental Section

Commercial iPP was obtained from Yanshan Petrol Co. (China), with a melt flow index of about 1.1 g/10 min (230 °C/2.16 kg, ASTMD 1238) and an average M_n and M_w of about 10^5 and 3.7×10^5 g/mol, respectively. The melting point is about 165 °C. Simultaneous WAXS and SAXS measurements were made using an in-house setup with a rotating anode X-ray generator (Rigaku RU-H300, 18 kW) equipped with two parabolic multilayer mirrors (Bruker, Karlsruhe), giving a highly parallel beam (divergence about 0.012°) of monochromatic Cu Kα radiation ($\lambda = 0.154$ nm). The SAXS intensity was collected with a two-dimensional gas-filled wire detector (Bruker Hi-Star). A semitransparent beamstop placed in front of the area detector allowed monitoring the intensity of the direct beam. The WAXS intensity was recorded with a linear position sensitive detector (PSD-50M, M. Braun, Germany), which could be rotated around the beam path to measure either in the meridianal or in the equatorial direction. The SAXS and WAXS intensities were normalized to the intensity of the direct beam.

A Linkam CSS450 temperature-controlled shear system was employed as sample stage. The glass windows were replaced by two brass plates with apertures covered by 50 μm thick Kapton foil for the X-ray beam. The iPP sample was held in the gap between the two windows and sheared by a single

* Corresponding author: e-mail dejeu@amolf.nl.

10.1021/ma025991a CCC: $25.00
Published on Web 06/07/2003

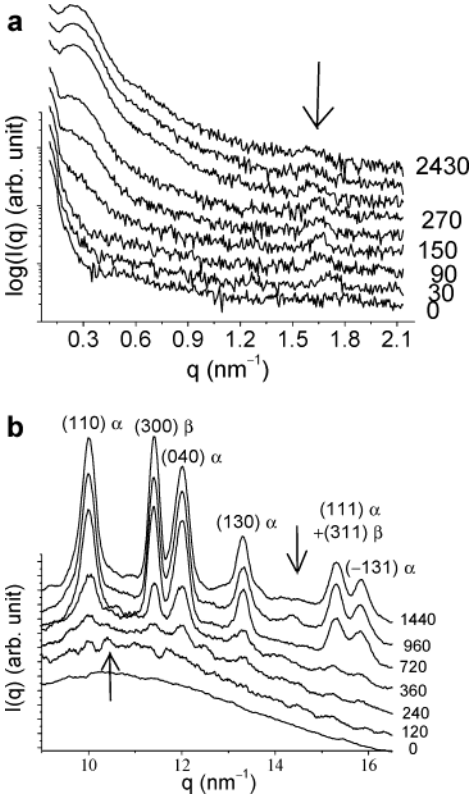

Figure 1. One-dimensionally integrated SAXS (a) and WAXS (b) patterns of iPP during crystallization at 140 °C after a step shear with a shear rate of 1 s^{-1} and a strain of 1500%. Numbers give the crystallization time in seconds; the arrows indicate the smectic scattering peaks.

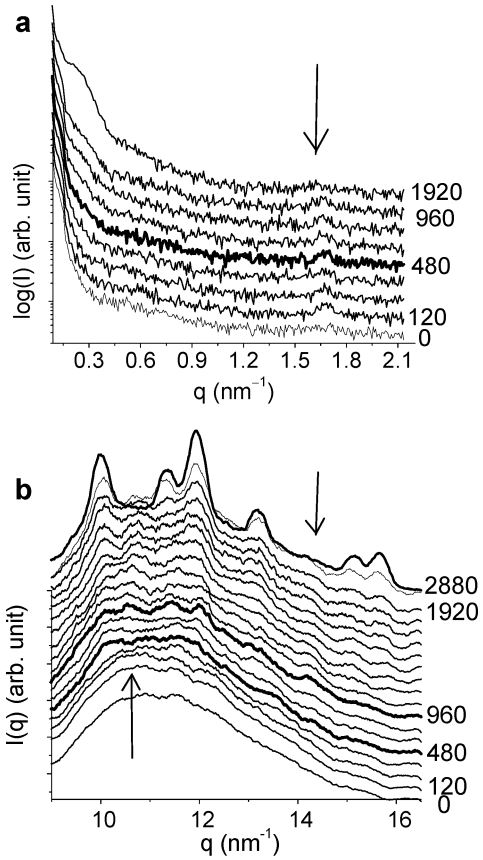

Figure 2. One-dimensionally integrated SAXS (a) and WAXS (b) patterns of iPP during crystallization at 150 °C (same conditions as in Figure 1).

rotation step of the bottom plate. A similar construction was described in ref 27. The samples were preshaped into thin disks with a thickness and a diameter of about 1.2 and 30 mm, respectively. Subsequently, they were pressed between the two plates at 210 °C to a gap of 1.0 mm. After the thickness adjustment the sample was cooled and cut to fit the diameter of the upper plate. For the actual measurements the sample was first melted at 210 °C for 10 min and then cooled to the crystallization temperature (140, 145, 150, and 155 °C) at a cooling rate of 30 °C/min. Upon reaching the crystallization temperature, a step shear was applied with shear rates between 0.5 and 30 s^{-1} at a fixed shear strain of 1500%. The whole process was monitored by SAXS and WAXS using 30 and 120 s/frame, respectively.

Results

The two-dimensional SAXS intensity was integrated azimuthally to obtain the scattering profile as a function of $q = (4\pi/\lambda) \sin \theta$, the modulus of the momentum transfer vector **q**, λ being the wavelength and 2θ the scattering angle. Figures 1a and 2a show the integrated SAXS pattern of iPP during crystallization after a step shear at 140 and 150 °C, respectively. A small peak around $q = 1.67$ nm^{-1} appears immediately after the step shear, while a clear indication of crystallization emerges around $q = 0.25$ nm^{-1} only after about 100 s (at 140 °C) and 480 s (at 150 °C). The shear-induced smectic phase does not emerge anymore above about 155 °C. The corresponding WAXS profiles in the equatorial direction are shown in Figure 1b and Figure 2b, respectively. Figure 2 shows essentially similar features as Figure 1 but provides more detailed information as at 150 °C the structural development is slower. During the first stage of the process (about 480 s, Figure 2b), an increase of the intensity of the equatorial amorphous halo is observed while the WAXS pattern does not indicate any crystalline scattering peak. This excludes that the small peak in the SAXS patterns originates from some crystalline form of iPP. Although at 480 s we observe a further increase of the WAXS intensity, clear scattering peaks only appear after about 960 s. In addition to the crystalline peaks corresponding to the α-form and the *β*-form, initially also two small peaks appear at $q \approx 10.6$ and $q \approx 14.3$ nm^{-1}, which subsequently disappear with time (see Figures 1b and 2b). These peaks could possibly be assigned as (113) and (117) of the *γ*-form.[31−33] However, the intensity of *γ*(113) is expected to be very low: 15% of *γ*(111), which is at the same position as α(110), and 17% of *γ*(117).[31] For short crystallization times (≤1600 s) the intensity at $q \approx 10.6$ nm^{-1} is in fact larger than at the *γ*(111) position. This supports the idea that the peak at $q \approx 10.6$ nm^{-1} mainly originates from the smectic structure, similar as found in fast quenched[20,21] or cold plasma-treated iPP samples.[22] This assignment is also favored by its disappearance at the end of the crystallization process. Such a behavior is not expected for a *γ*-form as solid−solid transformations between iPP modifications are difficult. On the basis of (i) the immediate appearance of a SAXS peak at $q = 1.67$ nm^{-1}, (ii) the absence of any crystalline scattering peak at early times, and (iii) the assignment of the peak at $q \approx 10.6$ nm^{-1}, we postulate that smectic ordering is produced by the step shear. In the following we shall refer to the peaks around $q = 1.67$ and $q = 0.25$ nm^{-1} in the SAXS pattern as the smectic peak and the crystalline peak, respectively, even though the structure leading to the first peak changes with crystallization time. During the

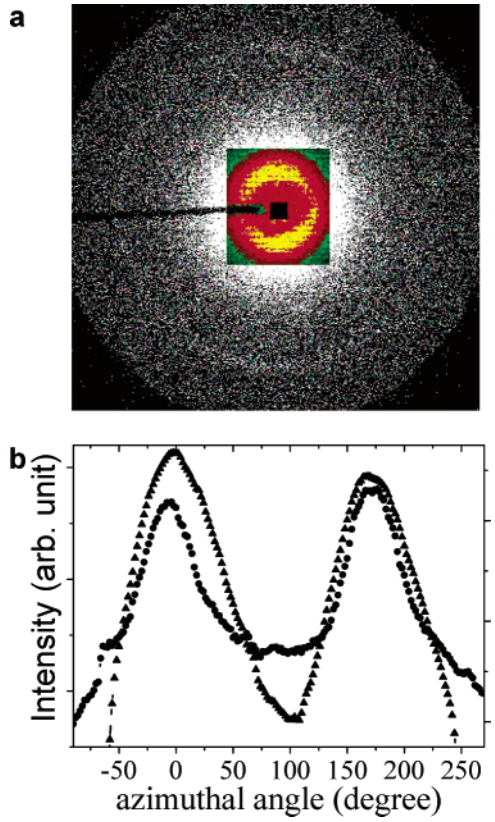

Figure 3. SAXS patterns of crystallized iPP induced by a step shear. (a) Two-dimensional pattern showing the orientation of the smectic and crystalline peaks; different scales are applied at low- and high-q regions for a better view. (b) Corresponding azimuthal distribution of the smectic peak (●) and the crystalline peak (▲). Zero corresponds to the vertical direction in (a).

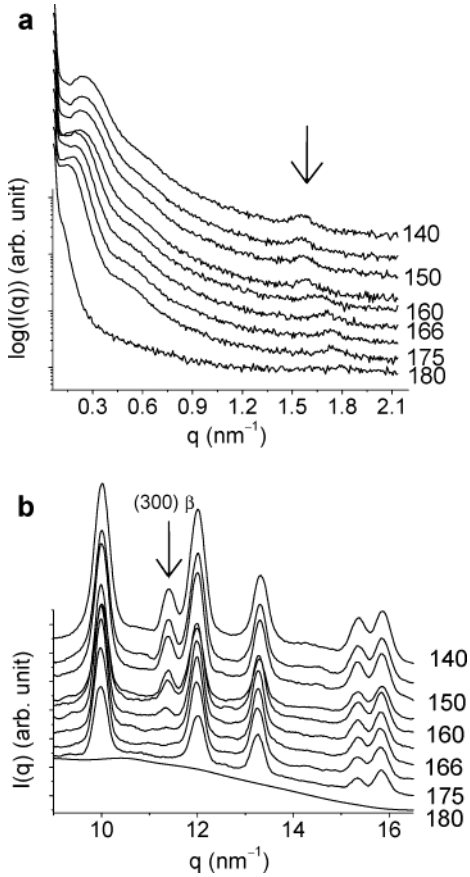

Figure 4. One-dimensional SAXS (a) and WAXS (b) patterns of shear-induced crystallized iPP during heating at 0.2 °C/min. Temperatures are indicated in °C.

crystallization process the smectic peak shifts continuously to slightly lower q values (finally about 1.62 nm^{-1}), but still much larger than the q value of the crystalline peak. In addition, the disappearance of two smectic WAXS peaks and the shift of smectic SAXS peak indicate the smectic regions also crystallize.

The two-dimensional SAXS pattern of the finally stage of crystallized iPP is shown in Figure 3a. The azimuthal distribution of the both the smectic and the crystalline peak is plotted in Figure 3b. We conclude that both the original smectic layers and the crystalline lamellae have the same orientation as the shear flow.

After completion of the crystallization, each sample was heated at a rate of 0.2 °C/min until melting occurred. The integrated SAXS and WAXS during this process are shown in Figure 4. With increasing temperature, the smectic peak initially shifts to slightly larger q values while its intensity decreases. At about 166 °C, the β-phase melts completely, as indicated by the disappearance of its (300) peak in the WAXS. Both the smectic and the crystalline SAXS peaks and the peaks associated with the α-phase in the WAXS disappear simultaneously around 180 °C. This melting behavior provides further evidence that the smectic regions have transformed into crystalline ones.

Figure 5a shows the integrated SAXS of iPP at 140 °C immediately after a step shear for different shear rates. The corresponding SAXS profiles after complete crystallization are shown in Figure 5b. For the applied variation of shear rates of about 2 orders of magnitude, the smectic period is approximately constant. Figure 6a shows for different shear rates the variation of the integrated SAXS intensity with crystallization time after a step shear. Plotting the resulting half-time of crystallization vs the intensity I of the smectic peak (Figure 6b) demonstrates explicitly a correlation between the smectic ordering and crystallization: clearly a larger value of I corresponds to faster crystallization. Assuming the nucleation to be proportional to I and the crystals to grow in three dimensions, the relation should correspond to a power law with an exponent equal to −3. This is the dashed line drawn in Figure 6b as a guide to the eyes. The assumption of three-dimensional growth is delicate as at the start of the crystallization the orientational ordering of the lamellar crystals is strong (80%). This would indicate an oriented thread nucleation model. However, at later stages the orientational ordering is lost and finally is only about 8%. In this situation the growth process does not have a strong preferred orientation anymore, and the assumption of three-dimensional growth is reasonable.

Discussion

Natta et al. proposed already more than 40 years ago the mesophase in quenched iPP to be smectic.[20] Though a great deal of work on the subject has been carried out since then, its structure and morphology are still a matter of controversy.[27,34−37] Values between about 4 and 10 nm were reported for the repetition period. Our SAXS and WAXS measurements provide conclusive evidence that the mesophase in iPP can indeed be described as a smectic layer structure, even though the nature of the in-plane ordering is not fully clear. The

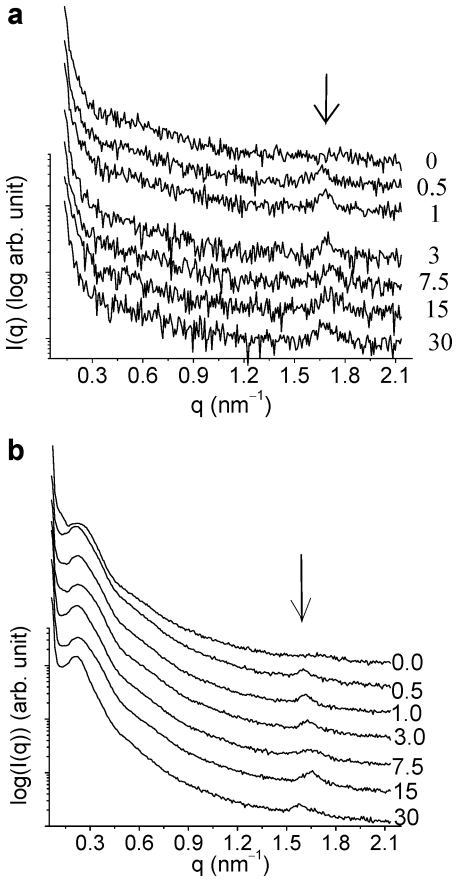

Figure 5. One-dimensional SAXS patterns of iPP at 140 °C after a step shear for different shear rates as indicated: (a) first frame of 30 s after the step shear; (b) final frame of 10 min after complete crystallization.

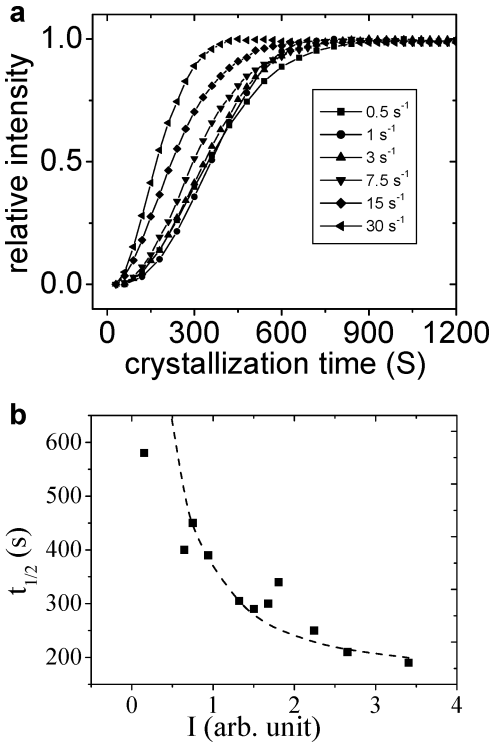

Figure 6. (a) Integrated intensity of SAXS vs crystallization time after a step shear with the same strain (1500%) at 140 °C. (b) Relation between the half-time of crystallization at 140 °C and the intensity of the smectic SAXS peak. The dashed line represents $y = a + bx^{-3}$. More data points are collected in (b) by repeated experiments.

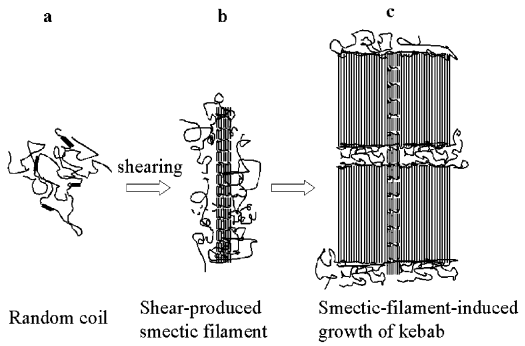

Figure 7. Schematic picture of shear-induced crystallization in iPP.

period of 3.8 nm is in remarkably good agreement with the value of about 4 nm estimated by Corradini et al.[21] from the width of a meridianal WAXS peak and is also close to the value of about 5.5 nm from ref 36. The controversy about the nature of the mesophase may be at least partly due to different thermal histories and consequently the presence of a mixture of smectic regions and nanocrystals. Contributions from the latter structures could lead to larger values of the period.[36] From our results we conclude that the smectic regions undergo a gradual transition to crystals, as indicated by a small shift to somewhat lower q values in the position of the smectic peak in the SAXS and the disappearance of the two smectic WAXS peaks. Note that this transition of the smectic regions is confined due to the presence of the surrounded lamellar crystals. It also indicates that at the crystallization temperature used the smectic structure is metastable, in agreement with the conventional view of the mesophase formed in iPP.

The smectic period is sensitive neither to variation of the shear rate (Figure 5) nor to the temperature (Figures 1 and 2). However, for temperatures above 155 °C no smectic ordering is observed anymore. This is attributed to both fast relaxation of the molecular chains at these high temperatures and to a decreased stability of the smectic phase. The length scale of about 3.8 nm corresponds to about 20 monomer units in a 3/1 conformation. It is not clear to us which underlying property could determine this value. From the limited width of our smectic SAXS peak the repetition must be at least several periods. According to estimates by Corradini et al.,[21] the width of the smectic regions is about 3 nm. In agreement with the weak intensity of the smectic WAXS peaks, we assume that this value approximately also applies to our situation. Hence, the smectic regions must be elongated: smectic bundles or filaments.

As liquid crystals are widely applied as nucleation agents,[38] we expect the smectic bundles to play the same role in iPP. This point is supported by (i) the correlation between the half-time of crystallization and the intensity of the smectic peak (Figure 6) and (ii) the coincidence of the orientation of the smectic layers and the final crystals (Figure 3). In Figure 7 a schematic picture is given to describe this process. Initially, the molecular chains of iPP are present as Gaussian coils (Figure 7a) in which some local helix may exist. After application of the step shear the chains are somewhat stretched. This creates a more pronounced helical structure that is aligned to form smectic bundles and gives the shish structure (Figure 7b). A shear field can also promote the appearance of smectic bundles at higher tempera-

tures similar to the case of the β phase.[39,40] As these bundles can be expected to have only relatively short helical sequences and a random hand due to the rapid organization process, they are not ready yet to form crystals. Subsequently, the oriented smectic bundles induce epitaxial crystal growth and the formation of kebabs (Figure 7c). Meanwhile, the smectic filaments themselves also slowly transform into crystals, with a slight increase of the period. The final result is the shish-kebab structure: the initial smectic filaments play the role of the shish, while the crystals epitaxially grown around it form the kebabs.

Three interesting points follow from the structural development as described. First, the smectic bundles promote surrounding crystallization as nucleation agents but do not easily transform into a crystalline structure. This implies coexistence of both kebab crystals and smectic filaments at the beginning of the crystallization process (Figure 2). These results support Lotz's arguments about the difficulty of helix inversion within an ordered structure.[10] The constraints imposed subsequently by surrounding lamellar crystals are another factor to slow down the transition from smectic order to crystal (see Figure 7c).

The second point regards the structure of the shish; from our results most probably it does not consist of extended-chain crystals. Although iPP is somewhat special because of its helical structure, this point is of general importance as in several semirigid polymers a mesophase has been observed under shear or drawing.[41,42] In these cases probably also a mesophase is involved in the shish while it may consists of defective microcrystals in some other polymers.[43] Then the picture of folded-chain crystals epitaxially grown around an extended-chain surface—used as a strong argument in favor of specific kinetic theories for the chain-folded model of crystallization[44]—is not appropriate anymore.

The third point is whether the growth scheme of Figure 7 can be generalized to standard quiescent conditions. Smectic filaments have been found in several rod-shaped colloid systems, such as fd viruses.[45] A model of formation and growth of smectic filaments similar to the Hoffman−Lauritzen model for polymer crystallization has been proposed recently by Frenkel and Schilling[46] and can be extended to iPP in a natural way. The result is that a single small smectic disk cannot grow but that this situation changes when other smectic disks with the same diameter are repeatedly added. This leads eventually to a smectic filament which becomes absolutely stable and can grow. This process indicates that smectic filaments can also develop without shear, and the model of Figure 7 could also be applicable to quiescent conditions.

When a smectic filament reaches a thickness $l^* = nd = 2\gamma_e/(\rho|\Delta\mu_c|)$, a crystal can grow epitaxially around it. Here n indicates the number of layers of thickness d, γ_e represents the free energy of the folded-chain surface, and $\Delta\mu_c = \mu_c - \mu_l$ is the difference in chemical potential between the crystal and the liquid phase.[47] For individual lamellae with their primary nucleus in the smectic filament, this picture of the critical nucleus is rather similar to the "fringed micelle" or "bundle" model.[48,49] In the case of smectic bundles entropic constraints on the smectic segments connected to the crystalline surface (used as an argument against this model for amorphous−crystalline interfaces[50]) are weak, leading a surface with a low free energy. Experimentally, the difference between μ_c and μ_s (the heat of transition from smectic to α-polymorph) is only about −0.6 kJ/mol.[51] Hence, for nucleation from smectic filaments the energy barrier is low, favoring fringed micelle nuclei. See also refs 52 and 53 for some recent reconsiderations of this concept. The question remains why we did not observe a clear smectic peak under quiescent conditions. We attribute this to a low number of regular helical sequences in the absence of shear. As a result, also the correlation length normal to the smectic layers will be relatively small.

Conclusion

In-situ SAXS and WAXS measurements indicate that smectic bundles are produced by a step shear in a supercooled isotactic polypropylene melt. The associated scattering peak at about $q = 1.67$ nm^{-1} appears immediately in the SAXS patterns before any formation of crystals. The period of the smectic mesophase is about 3.8 nm and depends neither on shear rate nor on temperature. Subsequently, crystals grow epitaxially around the smectic bundles, with a period that is about an order larger than the initial smectic one. Meanwhile, also the smectic filaments slowly transforms into crystalline ones, which leads to a slight increase of the period to about 4 nm. The precursor smectic bundles promote crystallization by acting as nucleation agent but cannot transform easily into a crystal itself. A new model of the shish-kebab structure is presented in which the initial smectic bundles (instead of extended-chain crystals) play the role of the shish, while the crystals grown epitaxially around it form the kebabs. A fringed-micelle type of nucleation is suggested for crystallization under both shear and quiescent conditions.

Acknowledgment. The authors thank B. Lotz (Strassbourg), D. Frenkel, T. Schilling, Y. Séréro, and M. Al-Hussein (Amsterdam) for valuable discussions and L. Zhang (East China Sci. & Tech. Univ.) for supplying iPP. This work is part of the Softlink research program of the "Stichting voor Fundamenteel Onderzoek der Materie" (FOM), which is financially supported by the "Nederlandse Organisatie voor Wetenschappelijk Onderzoek" (NWO).

References and Notes

(1) Armitstead, K.; Goldbeck-Wood, G. *Adv. Polym. Sci.* **1992**, *100*, 221.
(2) Strobl, G. *Eur. Phys. J.* **2000**, *E3*, 165.
(3) Imai, M.; Kaji, K.; Kanaya, T. *Phys. Rev. Lett.* **1993**, *71*, 4162.
(4) Ryan, A. J.; Fairclough, A.; et al. *Faraday Discuss.* **1999**, *112*, 13.
(5) Olmsted, P. D.; Poon, W. C. K.; Mcleish, T. C. B.; et al. *Phys. Rev. Lett.* **1998**, *81*, 373.
(6) Yeh, G. S. Y.; Geil, P. H. *J. Macromol. Sci., Phys. B* **1967**, *1*, 235.
(7) Yeh, G. S. Y.; Geil, P. H. *J. Macromol. Sci., Phys. B* **1967**, *1*, 251.
(8) Schultz, J. M.; Lin, J. S.; Hendricks, R. W.; Peterman, J.; Gohil, R. M. *J. Polym. Sci., Polym. Phys. Ed.* **1981**, *19*, 609.
(9) Cheng, S. Z. D.; Li, C. Y.; Zhu, L. *Eur. Phys. J.* **2000**, *E3*, 195.
(10) Lotz, B. *Eur. Phys. J.* **2000**, *E3*, 185.
(11) Muthukumar, M. *Eur. Phys. J.* **2000**, *E3*, 199.
(12) Pennings, A. J. *Crystal Growth*; Pergamon: Oxford, 1967; p 389.
(13) Miller, R. L. *Flow-Induced Crystallisation in Polymer Systems*; Gordon and Breach Science Publishers: New York, 1979.
(14) Hobbs, J. K.; Homphris, A. D. L.; Miles, M. J. *Macromolecules* **2001**, *34*, 5508.

(15) Liu, T. X.; Tjiu, W. C.; Petermann, J. *J. Cryst. Growth* **2002**, *243*, 218.
(16) Rueda, D. R.; Ania, F.; Balta Calleja, F. J. *Polymer* **1997**, *38*, 2027.
(17) Monks, A. W.; White, H. M.; Bassett, D. C. *Polymer* **1996**, *37*, 5933.
(18) Hu, W. B.; Fenkel, D.; Mathot, V. B. F. *Macromolecules* **2002**, *35*, 7172.
(19) Lotz, B.; Wittmann, J. C.; Lovinger, A. J. *Polymer* **1996**, *37*, 4979.
(20) Natta, G.; Peraldo, M.; Corradini, P. *Rend. Accad. Naz. Lincei* **1959**, *26*, 14.
(21) Corradini, P.; Petraccone, V.; De Rosa, C.; Guerra, G. *Macromolecules* **1986**, *19*, 2699.
(22) Poncin-Epaillard, F.; Brosse, J. C.; Falher, T. *Macromolecules* **1997**, *30*, 4415.
(23) Somani, R. H.; Yang, L.; Hsiao, B. S. *Physica A* **2002**, *304*, 145.
(24) Ran, S. F.; Zong, X. H.; Fang, D. F.; Hsiao, B. S.; Chu, B.; Philips, R. A. *Macromolecules* **2001**, *34*, 2569.
(25) Wang, Z. G.; Hsiao, B. S.; Srinivas, S.; Brown, G. M.; Tsuo, A. H.; Cheng, S. Z. D.; Stein, R. S. *Polymer* **2001**, *42*, 7561.
(26) Martorana, A.; Piccarolo, S.; Sapoundjieva, D. *Macromol. Chem. Phys.* **1999**, *200*, 531.
(27) Somani, R. H.; Hsiao, B. S.; Nogales, A.; et al. *Macromolecules* **2000**, *33*, 9385.
(28) Kumaraswamy, G.; Issaian, A. M.; Kornfield, J. A. *Macromolecules* **1999**, *32*, 7537.
(29) Kumaraswamy, G.; Kornfield, J. A.; Yeh, F. G.; Hsiao, B. S. *Macromolecules* **2002**, *35*, 1762.
(30) Seki, M.; Thurman, D. W.; Oberhauser, J. P.; Kornfield, J. A. *Macromolecules* **2002**, *35*, 2583.
(31) Bruckner, S.; Meille, S. V. *Nature (London)* **1989**, *340*, 455.
(32) Lotz, B.; Graff, S.; Staupe, C.; Wittmann, J. C. *Polymer* **1991**, *32*, 2902.
(33) Lotz, B.; Wittmann, J. C. *Prog. Colloid Polym. Sci.* **1992**, *87*, 3.
(34) Miller, R. L. *Polymer* **1960**, *1*, 135.
(35) Gomez, M. A.; Tanaka, H.; Tonelli, E. *Polymer* **1987**, *28*, 2227.
(36) Miyamoto, Y.; Fukao, K.; Yoshida, T.; Tsurutani, N.; Miyaji, H. *J. Phys. Soc. Jpn.* **2000**, *69*, 1735.
(37) Grebowicz, J.; Lau, J.; Wunderlch, B. *J. Polym. Sci., Polym. Symp.* **1984**, *71*, 19.
(38) Roetting, O.; Hinrichsen, G. *Adv. Polym. Technol.* **1994**, *13*, 57.
(39) Blundell, D. J.; Mahendrasingam, A.; Martin, C.; et al. *Polymer* **2000**, *41*, 7793.
(40) Gutierrez, M. C. G.; Karger-Kocsis, J.; Riekel, C. *Macromolecules* **2002**, *35*, 7320.
(41) Dhont, J. K. G. *Phys. Rev. Lett.* **1996**, *76*, 4269.
(42) Olmsted, P. D.; Lu, C. Y. D. *Phys. Rev. E* **1999**, *60*, 4397.
(43) Samon, J. M.; Schultz, J. M.; Hsiao, B. S.; et al. *Macromolecules* **1999**, *32*, 8121.
(44) Keller, A. Organization of the Macromolecules in the Condensed Phase. *Faraday Discuss. R. Soc. Chem.* **1979**, *68*, 145.
(45) Dogic, Z.; Fraden, S. *Phys. Rev. Lett.* **1997**, *78*, 2417; *Philos. Trans. R. Soc. London A* **2001**, *359*, 997.
(46) Frenkel, D.; Schilling, T. *Phys. Rev. E* **2002**, *66*, 041606.
(47) Wunderlich, B. *Macromolecular Physics*; Academic Press: New York, 1976; Vol. 2.
(48) Hermann, K.; Gerngross, O.; Abitz, W. *Z. Phys. Chem. (Munich)* **1930**, *B10*, 381.
(49) Flory, P. J. *J. Am. Chem. Soc.* **1962**, *84*, 2857.
(50) Grebowicz, J.; Lau. S. F.; Wunderlich, B. *J. Polym. Sci., Polym. Symp.* **1984**, *71*, 19.
(51) Zachmann, H. G. *Kolloid Z. Z. Polym.* **1969**, *231*, 504.
(52) Allegra, G.; Meille, S. V. *Phys. Chem. Chem. Phys.* **1999**, *1*, 5179.
(53) Kraack, H.; Deutsch, M.; Sirota, E. B. *Macromolecules* **2000**, *33*, 6174.

MA025991A